PLANT SCIENCE TODAY
ISSN 2348-1900 (online)
Vol 11(3): 236-244
https://doi.org/10.14719/pst.2701

HORIZON
e-Publishing Group
HePG

RESEARCH ARTICLE

In silico structural modeling of normal and mutated subunits of ADP-glucose pyrophosphorylase from *Triticum aestivum* to study protein-protein interactions

Saroj Rani[1], Aanchal Gupta[1], Deepshikha Kaushik[2], Sarvesh Rustagi[3], Sumira Malik[4], Rajesh Yogi[1]* & Nitesh Singh[5]*

[1]Department of UIBT-Biotechnology, Chandigarh University, Mohali-140413, India
[2]Centre for Bioinformatics, Maharshi Dayanand University, Rohtak-124001, India
[3]School of Applied and Life Sciences, Uttaranchal University, Dehradun-248007, India
[4]Amity Institute of Biotechnology, Amity UniversityJharkhand, Ranchi-(834002), India
[5]Faculty of Agricultural Sciences, Shree Guru Gobind Singh Tricentenary University, Gurugram-122505, India

*Email: rajeshyogi999@gmail.com; niteshigntu@gmail.com

OPEN ACCESS

ARTICLE HISTORY
Received: 23 June 2023
Accepted: 20 December 2023
Available online
Version 1.0 : 06 July 2024
Version 2.0 : 16 July 2024

Check for updates

Additional information

Peer review: Publisher thanks Sectional Editor and the other anonymous reviewers for their contribution to the peer review of this work.

Reprints & permissions information is available at https://horizonepublishing.com/journals/index.php/PST/open_access_policy

Publisher's Note: Horizon e-Publishing Group remains neutral with regard to jurisdictional claims in published maps and institutional affiliations.

Indexing: Plant Science Today, published by Horizon e-Publishing Group, is covered by Scopus, Web of Science, BIOSIS Previews, Clarivate Analytics, NAAS, UGC Care, etc
See https://horizonepublishing.com/journals/index.php/PST/indexing_abstracting

CITE THIS ARTICLE

Rani S, Gupta A, D Kaushik D, Rustagi S, Malik S, Yogi R, Singh N. *In silico* structural modeling of normal and mutated subunits of ADP-glucose pyrophosphorylase from *Triticum aestivum* to study protein-protein interactions. Plant Science Today. 2024; 11(3): 236-244. https://doi.org/10.14719/pst.2701

Abstract

ADP-glucose pyrophosphorylase is a heterotetrameric enzyme with pairs of large subunits (LS) and small subunits (SS) involved in starch biosynthesis. The increase in grain yield and plant biomass is brought about by the deregulation of endosperm. Thus, AGPase has attracted widespread interest in improving starch content in crop improvement. The data herein conclusively shows that mutation insertion involved in conformational changes is responsible for the decrease in a pocket in the mutated subunit. This type of conformational change might be beneficial for better protein-protein interaction. The present study is aimed to model and compare the structure of normal and mutated large subunits of wheat AGPase to study their structural differences. Mutations by insertion are involved in conformational changes that are responsible for the decrease in the pocket in the mutated subunit. Such conformational changes are often beneficial to study PPI (protein-protein interactions). Further investigations were carried out using docking studies to gain insight into interaction. Based on these studies, it may be suggested that such type of mutations are usually beneficial for starch production in wheat which is considered one of the significant Indian food crops.

Keywords

AGPase; homology modeling; secondary structure; small and large subunits; docking; *T. aestivum*

Introduction

Wheat (*Triticum aestivum*) is one of the significant Indian food crops. According to FAS New Delhi forecasts (https://www.fas.usda.gov/data/india-grain-and-feed-annual-6), India is marching towards a record wheat production in the marketing year 2022–2023 (April–March) with a record 110 million metric tons (MMT) from 30.9 million ha. Last year production in India was recorded at 109.6 MMT from 31.1 million ha. Considering the Russian-Ukrainian war which has disrupted the wheat supply chain from the Black Sea, Indian wheat is heading towards record exports. Wheat starch vote for 20% of the human calories and protein requirement (1, 2) in the world where 95% of food production depends on starch and *Ipomoea batatas* serves as a major source for extraction of starch (3).

Starch is a carbohydrate-polymer constituting linear and helical amylose, branched amylopectin, where glucose units are joined by glycosidic bonds (4–6). The physical component of starch strongly differs from glycogen, thereby getting cruciality for the increased importance of starch and its varied applications. Starch is abundantly found, cheap, non-toxic and biodegradable for various food and non-food industries; having huge usage in dairy, bakery goods and meat products (7, 8). Four enzymes: starch synthase, ADP-glucose pyrophosphorylase (AGPase), starch de-branching enzyme and starch branching enzyme are known to play an imperative role in starch biosynthesis (9,10), which involve 3primarysteps, described as activation of glucose residues, elongation of chain and synthesizing side chains (11–13).

AGPase is tissue-specific and encoded by two different genes, Shrunken-2 (Sh2) and Brittle-2 (Bt2). AGPase has a heterotetramer structure, with 2 small/catalytic subunits (SS) encoded by Bt2 and 2 large/modulatory subunits (LS) encoded by Sh2 (14); plays a crucial role in the regulation of glycogen and starch biosynthesis pathways in bacteria and plants respectively. In the starch biosynthetic pathway, AGPase converts glucose-1-phosphate and ATP to ADP-glucose and pyrophosphate (PPi) (15, 16). ADP-glucose further serves as a glucosyl donor for the synthesis of glucan by starch synthase enzyme. The wheat endosperm is composed of about 70% starch and wheat starch serves as a major storage carbohydrate, containing about 60–75% grain and 70–80% flour (17, 18).

Starch quality is largely evaluated by considering the amylose to amylopectin ratio (19). The number and weight of seeds are crucial yield components of wheat grain and new approaches are continuously required for the improvement of grain yield (20, 21). Although previously the yield of grains has been consistently enhanced by higher grain number per unit area, the conflict between average grain weight and grain number has become an impediment to grain yield improvement (21).

Wheat yield can potentially be improved by increasing individual grains' weight but such practices to increase grain yield by increasing grain size have been cramped by the existing negative correlation between grain weight and number (22–25).

Genetic studies have been recently used for the identification of QTLs (Quantitative trait loci) which are associated with size of grain in wheat and other similar crops (26, 27). For instance, an increase of 6.9% in grain weight has been shown in isogenic lines of wheat that carried a QTL on Chr 5A (28); whereas the greatest hike of 20% in grain weight was observed in triple mutant lines of TaGW2 gene (29). But we cannot ignore that all such cases of increased grain weight always had a little impact on the yield of grain due to their negative correlation (30–32).

In the current study, the crystal structure of the small subunits of potato tubers was used as a template to model the 3D structure of the normal and mutant subunits of wheat AGPase *in silico* homology. We further analyzed and overlaid the predicted 3D structures of the major subunits of normal and mutant AGPase in wheat. Molecular docking studies were performed to gain insight into the interactions between the subunits.

Materials and Methods

Sequence retrieval

The protein sequences of AGPase large (522 amino acids) and small subunits (473 amino acids) of wheat were retrieved from the NCBI's (National Center for Biotechnology Information) protein database (https://www.ncbi.nlm.nih.gov/protein). The suitable template was obtained using the primary amino acid sequence. A homology search using BLAST-P was performed against the Protein Data Bank to generate a 3D coordinate structure. The crystal structure of potato AGPase (1YP2) available at PDB was used as a modeling template and Clustal W was used for conducting sequence alignment between the model and template sequence.

Structure prediction and validation

The Secondary structure properties of the protein were computed by using Jpred 4 (http://www.compbio.dundee.ac.uk/jpred4/index.html). Homology models of large and small subunits were built using ModBase (https://modbase.compbio.ucsf.edu). The mutated large subunit was also modeled. The best models were developed, optimized and evaluated. The quality and authentication of the subsequent models were performed using PROCHECK, ERRAT and VERIFY3D from UCLA-DOE LAB — SAVES v6.0 (https://saves.mbi.ucla.edu/). The model was also analyzed in SuperPose (http://superpose.wishartlab.com/). The overall stereochemical properties of the protein were evaluated using the Ramachandran plot analysis provided by PROCHECK. The surface topology was determined by the CastP server (http://sts.bioe.uic.edu/castp/index.html?3igg). The folding states of AGPase large and small subunits from wheat were predicted by the Fold Index program (https://fold.proteopedia.org/cgi-bin/findex).

Protein-protein interactions

The refined protein model was used to study the protein-protein interactions. Docking analysis was performed by GRAMM-X molecular docking tool (http://vakser.bioinformatics.ku.edu/resources/gramm/grammx). The selected models of large and small subunits were docked and the best hydrophobic and electrostatic models were selected, and the final model, concerning the total score, was selected for further analysis. The Ligplot+ v2.2 program (https://www.ebi.ac.uk/thornton-srv/software/LigPlus/) was used to analyze hydrogen and hydrophobic interactions between two subunits.

Results and Discussion

Template identification

The highest homology was observed with potato ADP glucose pyrophosphorylase using BLAST analysis. Alignment between wheat, rice and maize ADP glucose pyrophos-

phorylase sequences (Fig. 1) revealed a conserved pattern of 6residues that differed in only one residue. Using the potato AGPase template (1YP2), Modbase was used to model the highly mutated subunits of wheat and the final model was selected based on the DOPE score.

Predicting 3D structure and validation

Recent developments in the field of computational biology have properly condensed the cost and time of experiments in predicting the structure and function of proteins. One of the best methods for protein structure modeling is sequence comparison, which requires structure prediction i.e., sequence of interest, with a sequence of known structures available in the database. Based on the BLAST analysis PDB ID: 1YP2 i.e., potato AGPase was considered to be the best template structure for the relative model building of wheat AGPase. The template had the highest %of amino acid sequence identity and was shared with the target sequence. The model with the lowest DOPE value was considered thermodynamically stable from the various models generated and was selected for improvement and validation. The quality of the model was verified with the

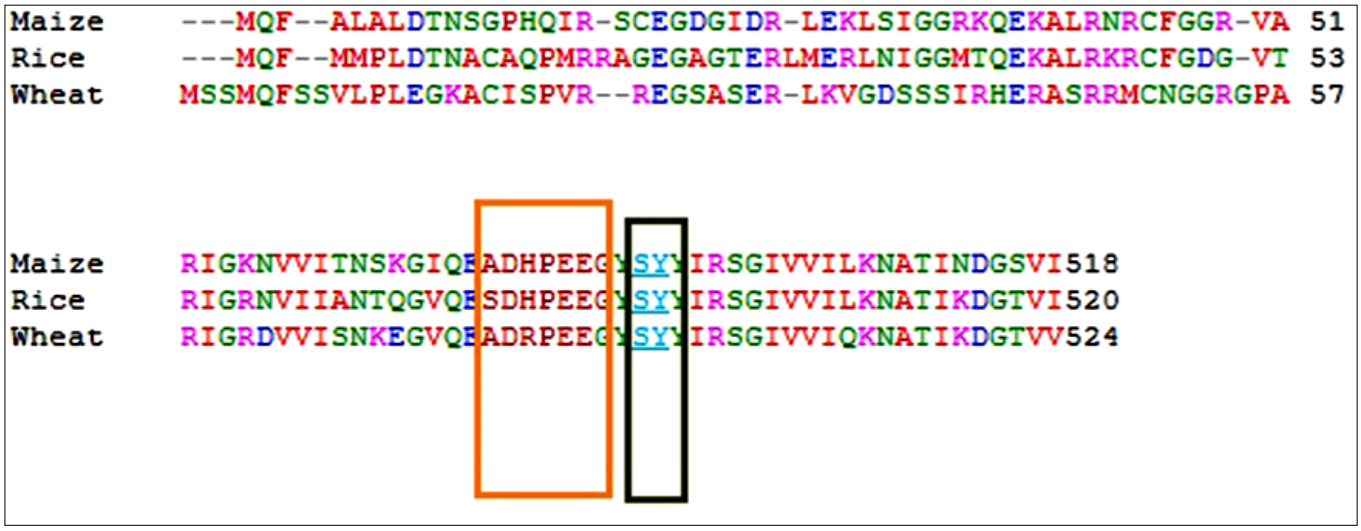

Fig.1. Sequences of 6-residue in maize (**ADHPEE**), rice (**SDHPEE**) and wheat (**ADRPEE**) appeared immediately before serine (**S**) and tyrosine (**Y**) insertion sites (underlined).

Secondary structure analysis

The comparative analysis of the secondary structure of normal and mutated subunits of wheat AGPase showed an absence of secondary structure elements in the mutated subunit compared to the normal one (Fig. 2).

These results showed that a small portion of the secondary structure of the 6 amino acid residues immediately preceding the insertion site of additional amino acids (serine and tyrosine) was reduced in mutant maize but not in mutant rice.

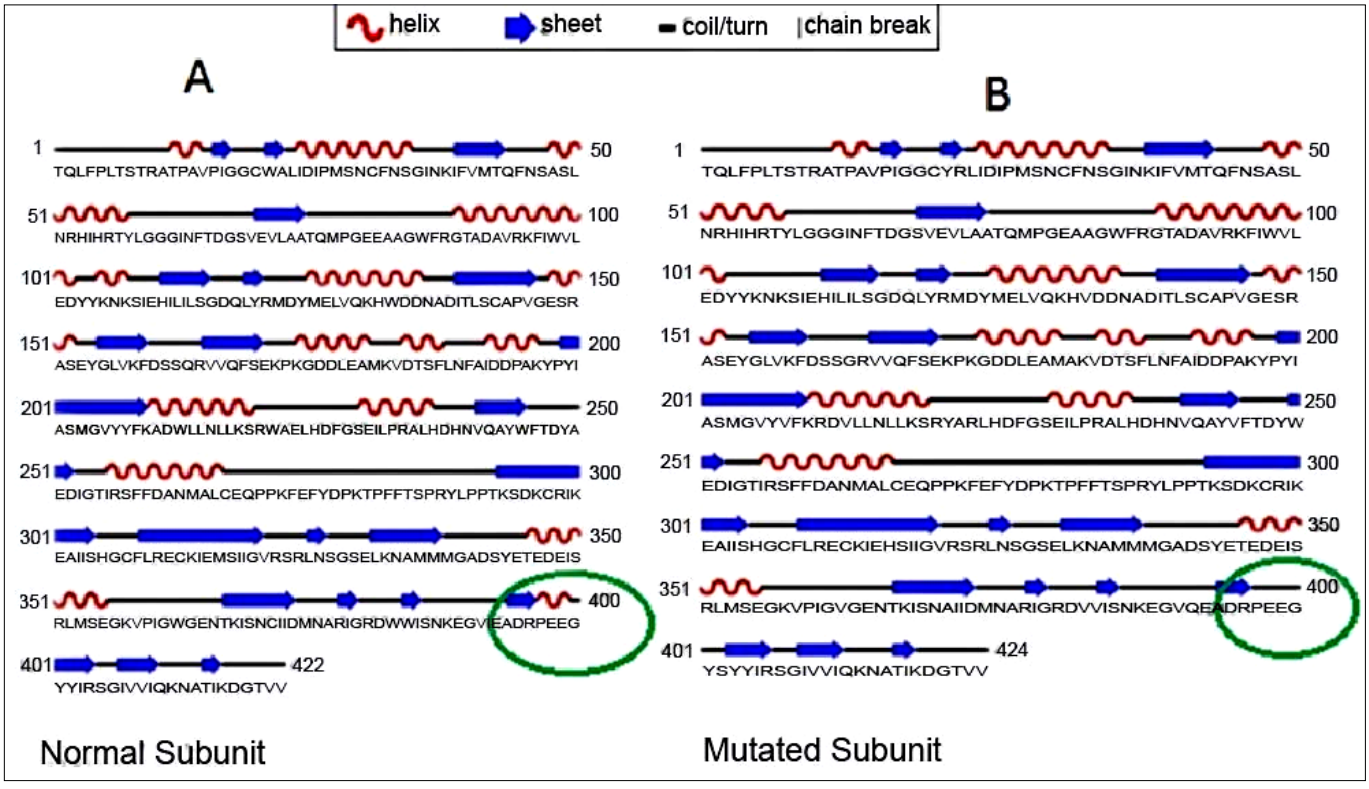

Fig. 2. Graphical representation of the secondary structures of **A**) normal as well as; **B**) mutated subunit of ADP glucose pyrophosphorylase in wheat, there is loss of secondary structure elements in the mutated subunit.

Structural Analysis and Verification Server (http://nihserver.mbi.ucla.edu/SAVES/). The main parameters recorded by SAVES were Ramachandran plot analysis, peptide bond planarity, side-chain parameters, backbone bond length and overall quality factor (ERRAT). The stereochemical quality of the predictive model and the accuracy of the protein model were evaluated after the improvement process using the Ramachandran map calculation within PROCHECK.

Modeled structure of normal large and small subunits of AGPase has been shown in Fig. 3a and Fig. 4a respectively of which the green color structure is a helix, blue is a sheet and red is the loop. The Ramachandran plot predicted by the SAVES analysis is shown in Fig. 3b. In the Ramachandran plot, the highest quality model is expected to contain more than 90% amino acids in the most preferred regions (27). In the generated model, it was found to be 87.6% in LS (Fig. 3b) and 92.2% in SS (Fig. 4b) suggesting the high quality of the models. The PROVE analysis revealed RMS Z-score was almost equal to 1 for the high-quality model while in our generated model the value of the large subunit of AGPase was 1.40 and for small subunit the value was 1.33 (Fig. 2d) and (Fig. 4d). The modeled structure of the mutated large subunit of Wheat AGPase is shown in (Fig. 2e) as proposed by ERRAT; the general quality factor was 67.15 for LS (Fig. 2c) and 75.744 for SS of AGPase (Fig. 4c) the high-resolution structures usually produce a value of around 95%. Although the result of ERRAT program was not favorable, still we considered that these are of good quality while the rest of the other para-

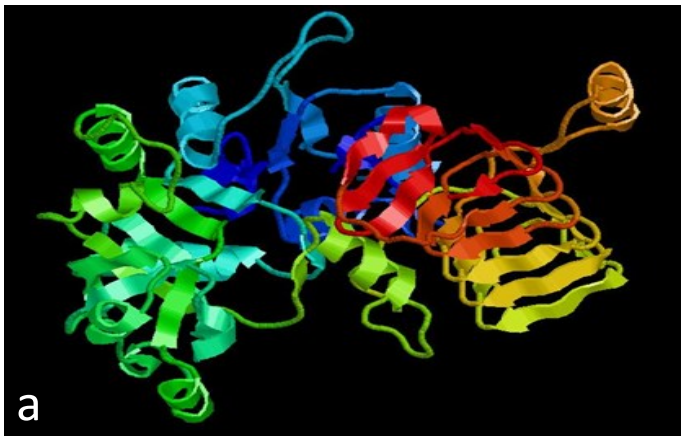

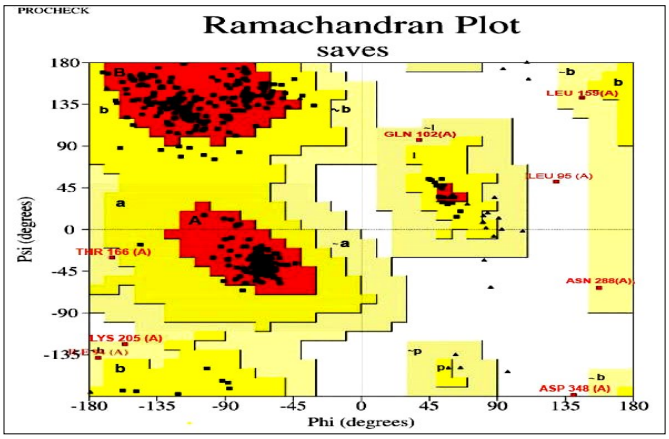

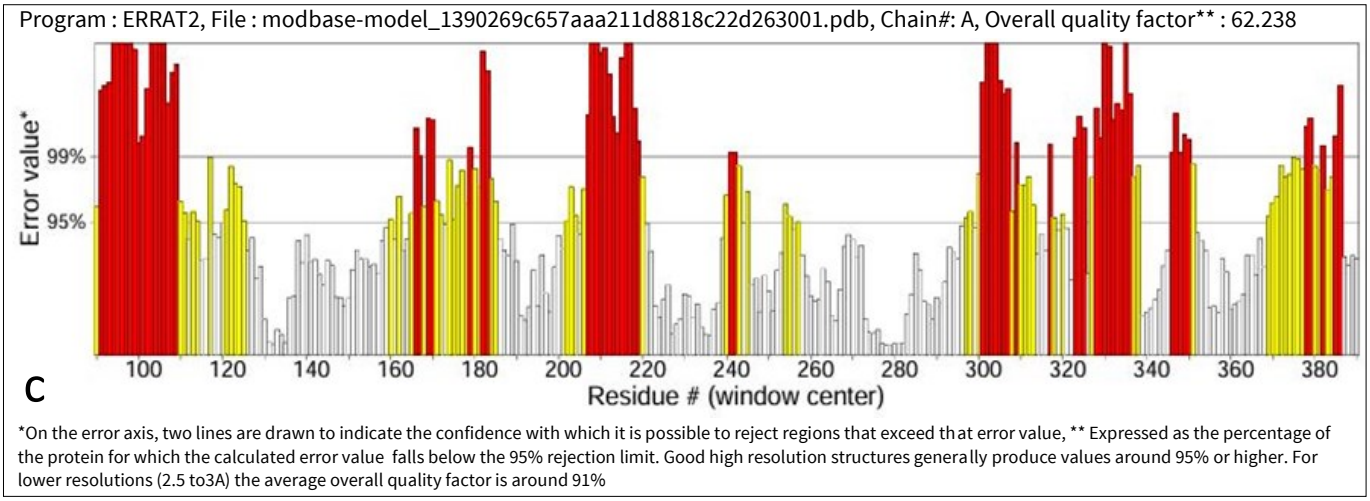

*On the error axis, two lines are drawn to indicate the confidence with which it is possible to reject regions that exceed that error value, ** Expressed as the percentage of the protein for which the calculated error value falls below the 95% rejection limit. Good high resolution structures generally produce values around 95% or higher. For lower resolutions (2.5 to3A) the average overall quality factor is around 91%

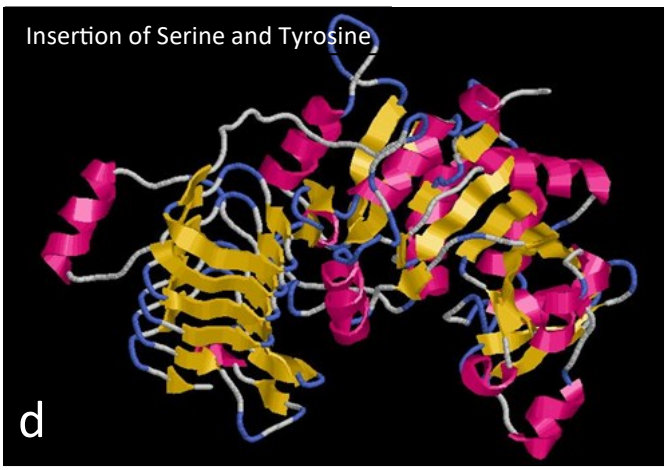

Fig. 3. a) The resulting model for AGPase (LS) generated by Modbase Server.; **b**) Quality assessment of 3D model of LS of AGPase evaluated by Ramachandran plot: red region in the graph specifies the most allowed regions, whereas yellow regions denote allowed region; **c**) ERRAT shows the model quality of 62.238%; **d**) Modelled structure of Mutated (LS) here arrow shows the site of insertion of serine and tyrosine.

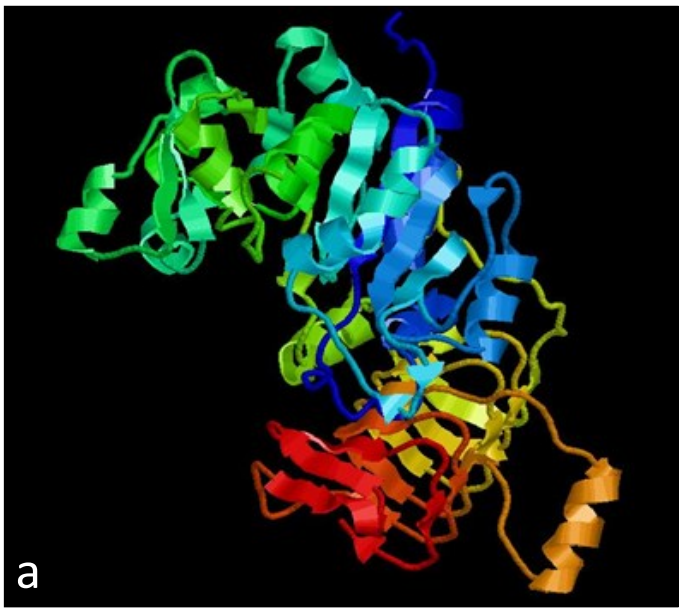

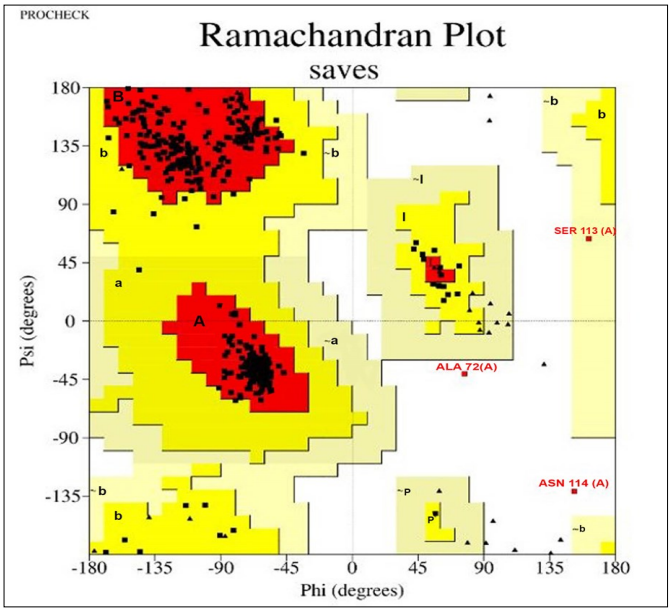

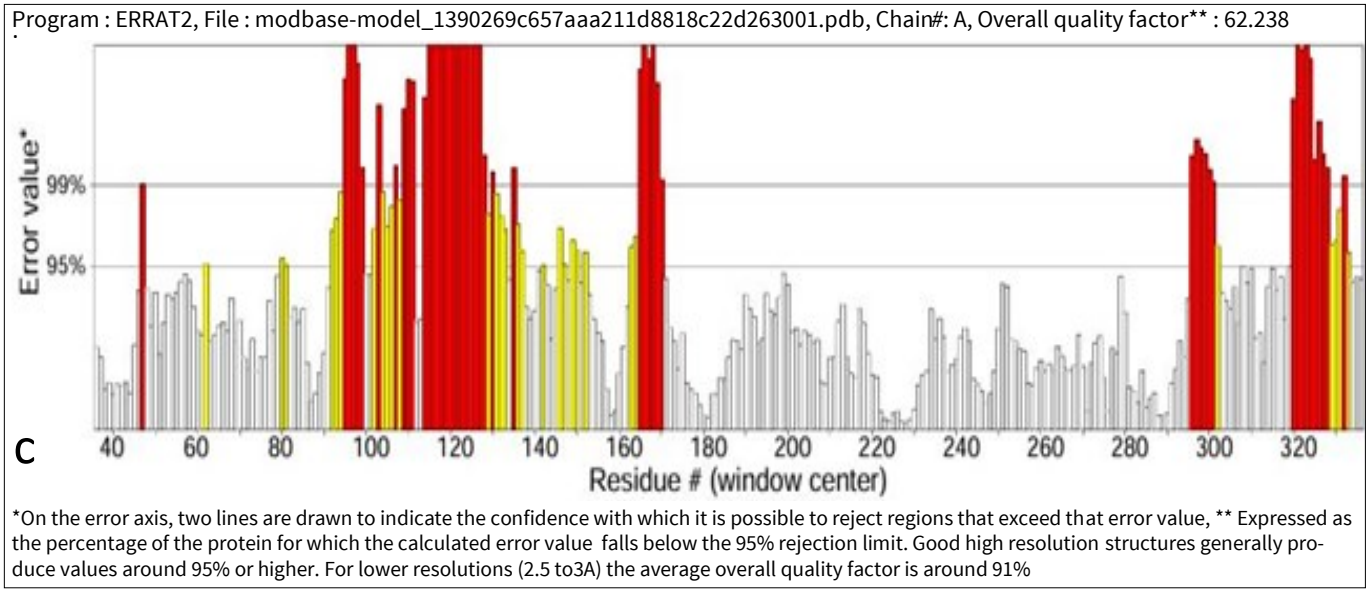

Fig. 4. a) The resulting model for AGPase (SS) generated by Modbase; **b**) Quality assessment of 3D model of SS of AGPase evaluated by Ramachandran plot: Red region in the graph specifies the most allowed regions, whereas yellow regions denote allowed region; **c**) ERRAT shows the model quality of 76.959 %.

meters were favorably demonstrating that it is a reasonably good quality model (Fig. 3c and 3d) The resulting model for AGPase (LS) generated by Modbase, here yellow arrow, shows the six-element long secondary structure which is present in normal subunit but absent in mutated form. This result had consistency with earlier predictions. Previous investigation observed that number of allelic missense and nonsense OsAGPL2 mutants was generated by using TILLING (Targeting Induced Local Lesions in Genomes) and N-methyl-N-nitrosourea (MNU) with treatment of fertilized egg cells (32). It's interesting to note that the significantly shrivelled seeds from three of the missense mutants—two of which included T139I and A171V—had starch content and seed weight that were comparable to the shrivelled seeds from OsAGPL2 null mutants.

Identification of binding pockets

CASTp was used for visualization of the annotated functional residues, with emphasis on mapping surface pockets and interior voids. It can identify functionally important residues and provide a complete understanding of the structural basis of protein function. The 2 best binding pockets with a high area and volume, one with an area of 2303.1 and a volume of 3755.5 (Table 1), were predicted by CASTpas active sites. Based on this prediction 2 conserved binding pockets appeared to be likely active sites for the docking study as shown in Supplementary Fig.1..

The Fold Index of (a) LS AGPase and (b) SS AGPase were plotted with a window size of 51, and the plot shows that it contains native-state unstructured regions. Positive and negative numbers represent ordered and disordered proteins respectively. Amino acids proposed as ordered are shown in green and unordered amino acids are shown in red respectively (Fig. 5.1). Table 2 and Fig. 5.2 present a

Table 1. Prediction of the surface topology of AGPase subunits by CastP server.

Crop	Number of Pockets	Area Å 2	Volume Å 3
Wheat (LS) Normal	82	2303.1	3755.5
Wheat (LS) Mutated	68	2878.8	654.5
Wheat (SS)	48	1573	2215.4

LS-Large subunit; **SS**-small subunit

summary of results obtained from Fold Index. More number of disordered regions (6) were found in AGPase SS as compared to AGPase LS (2) whereas the longest disordered region was found in LS is 47 and SS is 17. The number of disordered residues in LS was 56 and SS was57. In a normal large subunit of AGPase, the number of pockets was 82 but when we inserted a mutation at the particular site, the number of pockets was reduced from 82 to 68. Due to the insertion of mutation, there were conformational changes that could be responsible for a decrease in the pocket in the mutated subunit. This type of conformational change might be beneficial for better protein-protein interaction. So it could be suggested that such type of mutation might be beneficial for the enhancement of starch production in wheat also but this still requires further validation through a wet lab approach.

Protein structure and docking

Amino acids (GLN269, LYS 293, LYS 293, ASP 295 ILE299, GLUA 301 ALA302) of normal AGPase-L were found to form hydrogen bonds with amino acids (ARG 292, THR 266, ASP300, ASP 300, CYS296, GLU294 and LEU 293) of AGPase-S (Supplementary Fig. 2).

The total number of hydrogen bonds formed was

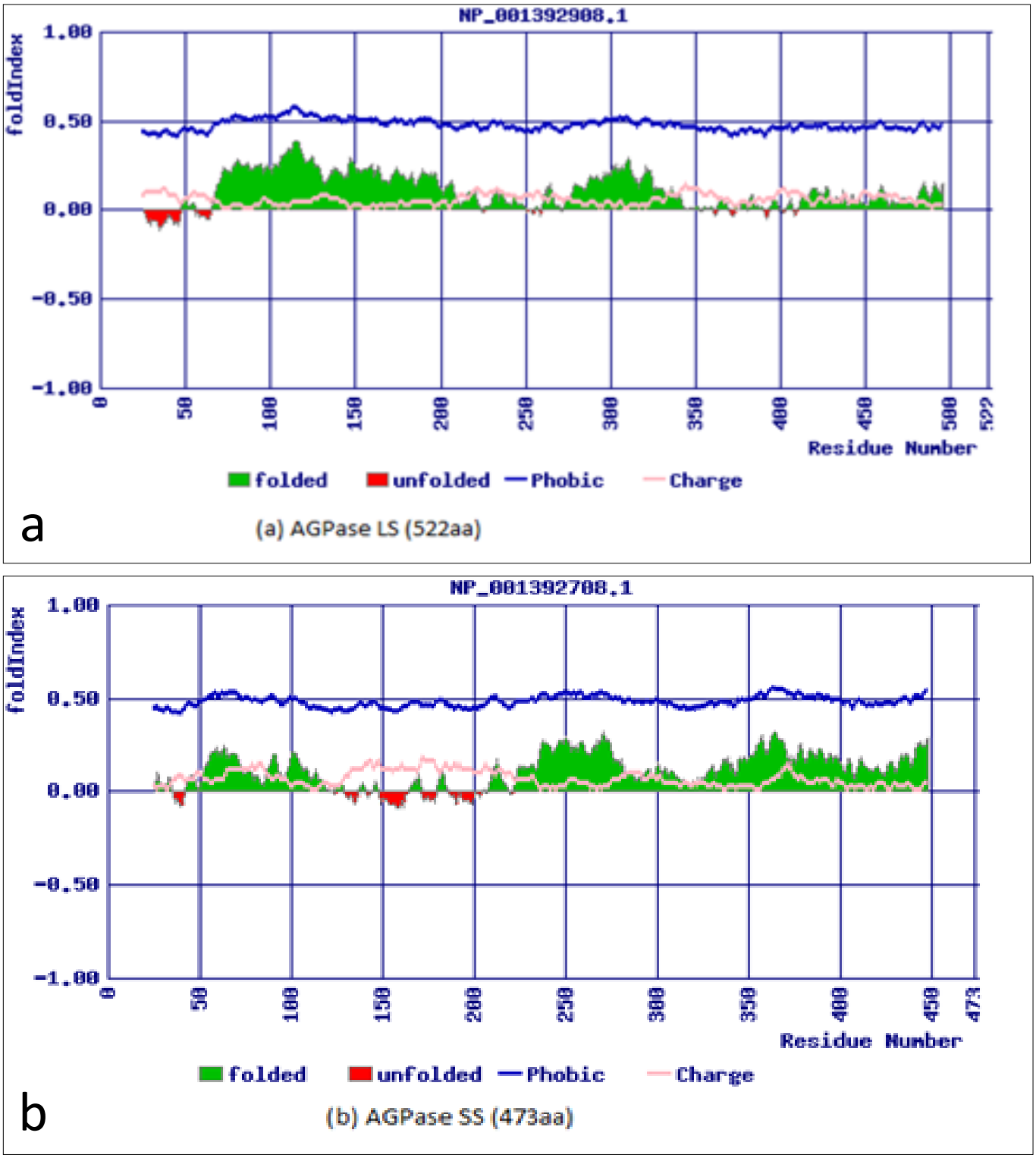

Fig. 5.1. Fold Index: Glucose-1-Phosphateadenyltransferase **a**) LS-AGPase (Accession No. NP_001392908, 522 residues, unfoldability 0.154, charge 0.010, Phobic 0.472) **b**) SS AGPase (Accession No. NP_001392708.1, 473 residues, unfoldability 0.150, charge 0.027, Phobic 0.477) plotted with window size 51.

Table 2. Summary of Fold Index results.

AGPase	Large Subunit	Small Subunit
Number Disordered Regions	2	6
Longest Disordered Region	47	17
Number Disordered Residues	56	57
Predicted disorder segments	[1]- [47] length: 47 score: -0.06 ± 0.02 [56]- [64] length: 9 score: -0.04 ± 0.01	[36]- [41] length: 6 score: -0.06 ± 0.02 [128]-[137] length: 10 score: -0.03 ± 0.02 [148]-[164] length: 17 score: -0.05 ± 0.03 [171]-[178] length: 8 score: -0.04 ± 0.01 [187]-[191] length: 5 score: -0.04 ± 0.02 [193]-[203] length: 11 score: -0.04 ± 0.02

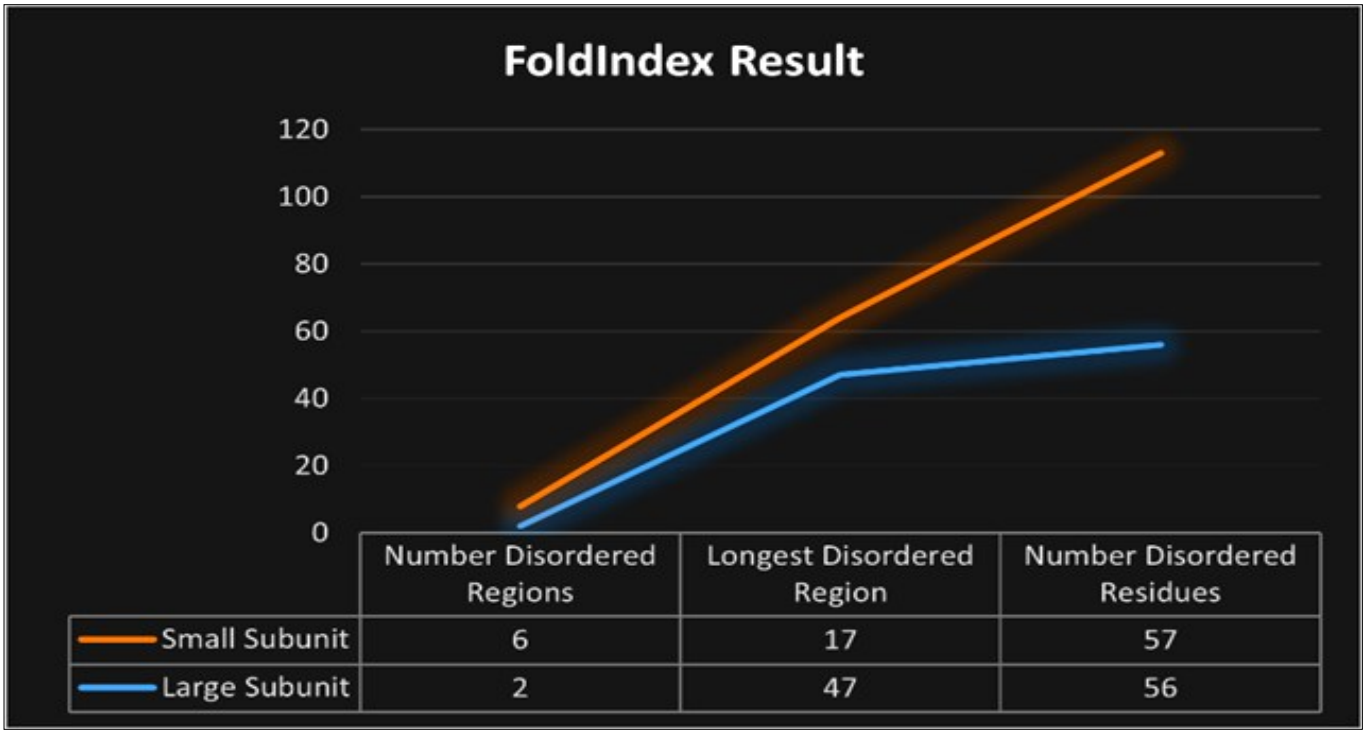

Fig. 5.2. Graph depicting comparative analysis of results obtained from Fold Index.

16, out of this only seven were having a bond distance of less than 3.00 Å. In the case of the mutated subunit, the amino acids involved in interaction were CYS 267, THR 284, THR 292 and LYS293, of the large subunit and ASP 295 with LYS 317, HIS312, ILE 328, THR 290 and ASP 325 of the small subunit of AGPase. In this total number of H-bond formed were also 16 but out of this only 6 were having bond distances less than 3.00 Å (Table 3).

In addition, some amino acids in AGPase-L were involved in the formation of hydrophobic contacts with the amino acids in (SS) AGPase. This indicates that the complex is stabilized by both hydrogen bonds and hydrophobic interactions. Only 2 of the below amino acids were proven to be important. The large subunit amino acid LYS293 provides hydrogen bonds to the small subunit ASP300 at the smallest 2.22 Å intervals in the complex. Multiple alignments revealed the 6-residue sequence ADHPEE of maize, SDHPEE of rice and ADRPEE of wheat just before the insertion site of serine (S) and tyrosine (Y). Top-of-form and bottom-of-form comparison of the secondary structure of normal and mutated subunits of wheat AGPase showed that there is an absence of secondary structure elements in the mutated subunit as compared to the normal one (Fig. 2). In the case of mutant maize, the long secondary structure segment of 6 amino acid residues immediately before the insertion site of additional amino acids (serine and tyrosine) was reduced instead of the mutant rice. BLAST analysis revealed that the template with the highest % of amino acid sequence identity with the target sequence was potato AGPase which is 1YP2.

Two best binding pockets with a high area of band 1, an area of 2303.1 and a volume of 3755.5 (Table 1) were predicted by CASTp to be active sites (Supplementaty Fig. 1). Depending on the CASTp calculation, these 2 binding pockets appear to be potential active sites for docking analysis. Docking studies revealed that in a normal complex 2 amino acids were crucial, LYS 293 of the large subunit donates the hydrogen bond to ASP 300 of the small subunit with 2.22 Å distances which were the smallest in the complex. While in the case of the mutated complex, crucial amino acids were LYS 293 of the large subunit and THR 290 of the small subunit.

Conclusion

In crops such as wheat, there is an energy trade-off

Table 3. Hydrogen bonding patterns in normal and mutated large and small subunit complexes of AGPase.

Normal Large and Small Subunit					Mutated Large and Small Subunit				
Donor		Acceptor		Distance (Å)	Donor		Acceptor		Distance (Å)
ARG B	292	**GLN A**	269	2.58	**LYS B**	317	**CYS A**	267	2.97
ILE B	303	**THR A**	292	3.23	**HIS B**	312	**THR A**	284	2.34
THR A	292	**ILE B**	303	3.34	**ILE B**	328	**THR A**	292	2.75
LYS A	293	**THR B**	266	2.31	**THR A**	292	**ILE B**	328	2.76
LYS A	293	**ASP B**	300	2.22	**LYS A**	293	**THR B**	290	2.09
ASP B	300	**SER A**	294	3.18	**SER B**	326	**SER A**	294	3.21
SER A	294	**ALA B**	301	3.3	**SER A**	294	**SER B**	326	3.02
ASP B	300	**ASP A**	295	2.94	**ASP B**	325	**ASP A**	295	2.72
ILE B	298	**CYS A**	297	3.08	**VAL B**	323	**CYS A**	297	3.23
CYS A	297	**ILE B**	298	3.07	**CYS A**	297	**VAL B**	323	3.05
CYS B	296	**ILE A**	299	2.84	**ALA B**	321	**ILE A**	299	3.19
ILE A	299	**CYS B**	296	2.99	**ILE A**	299	**ALA B**	321	3.22
GLU A	301	**GLU B**	294	2.53	**GLU A**	301	**LEU B**	319	3
LEU B	293	**ALA A**	302	2.88	**VAL B**	318	**ALA A**	302	3.29
ALA A	302	**LEU B**	293	3.03	**SER B**	316	**ILE A**	304	3.04
ILE A	304	**ALA B**	291	3.18	**ILE A**	304	**SER B**	316	3.13

A-Large subunit; **B**-small subunit.

between grain weight and grain number regarded as 2 entities; as a result, most genes that improve grain weight also decrease grain number simultaneously. The current work attempted to model and compare the structural changes between the normal and mutant large subunits of wheat AGPase. When we introduced a mutation at a specific location, the number of pockets in an AGPase large subunit that was normally 82 decreased to 68. In order to see interaction, more research was done using docking studies. Based on this study, it might be suggested that such types of mutations could prove to be beneficial for the enhancement of starch production in wheat which will be a significant factor in satisfying the food requirements of developing nations like India but further validation through a wet lab approach is always mandatory.

Acknowledgements

The authors are thankful to the Director, ICAR-IIWBR, and Dr. J Kaushik, NDRI, Karnal for providing facilities for this work. This research received no specific grant from any funding agency.

Authors' contributions

SR and RY prepared the original draft. DK, SD and NS analyzed the data obtained. AG, SR, DK further reviewed and edited the manuscript. All authors approved the final draft of the manuscript after they had reviewed the findings.

Compliance with ethical standards

Conflict of interest: The authors declare that they have no conflict of interest.

Ethical issues: None.

References

1. Calderini DF, Castillo FM, Arenas MA, Molero G, Reynolds MP, Craze M *et al*. Overcoming the trade-off between grain weight and number in wheat by the ectopic expression of expansin in developing seeds leads to increased yield potential. New Phytol. 2021; 230(2):629-40. https://doi.org/10.1111/nph.17048
2. Kumar R, Mukherjee S, Ayele BT. Molecular aspects of sucrose transport and its metabolism to starch during seed development in wheat: A comprehensive review. Biotechnol Adv. 2018;36:pp. 954-67. https://doi.org/10.1016/j.biotechadv.2018.02.015
3. Altemimi AB. Extraction and optimization of potato starch and its application as a stabilizer in yogurt manufacturing. Foods. 2018;7:14. https://doi.org/10.3390/foods7020014
4. Precha-atsawanan S, Puncha-arnon S, Wandee Y. Physicochemical properties of partially debranched waxy rice starch. Food Hydrocol. 2018;79:71-80. https://doi.org/10.1016/j.foodhyd.2017.12.014
5. Singh N, Jiwani G, Rocha LS, Mazaheri R. Bioagents and volatile organic compounds: An emerging control measures for rice bacterial diseases. Bacterial Diseases of Rice and Their Management. 2023 May 5;255-74. https://doi.org/10.1201/9781003331629
6. Singh N, Pandey R, Chandraker SK, Pandey S, Malik S, Patel D. Use of wild edible plants can meet the needs of future generation. In: Agro-biodiversity and Agri-ecosystem Management. Singapore: Springer Nature Singapore. 2022 Jul 16;pp. 341-66. https://doi.org/10.1007/978-981-19-0928-3_18
7. Apriyanto A, Compart J, Fettke J. A review of starch, a unique biopolymer - Structure, metabolism and in planta modifications. Plant Sci. 2022;318:111223. https://doi.org/10.1016/j.plantsci..111223
8. Srivastava RP, Kumar S, Singh L, Madhukar M, Singh N, Saxena G *et al*. Major phenolic compounds, antioxidant, antimicrobial and cytotoxic activities of *Selinum carvifolia* (L.) collected from different altitudes in India. Frontiers in Nutrition. 2023;10.https://doi.org/10.3389/fnut.2023.1180225

9. Dixit P, Singh N, Singh L, Srivastava RP, Pandey S, Singh S *et al.* Screening for the biochemical profile and biological activity in *Cephalotaxus* and *Taxus* collected from North-Eastern Himalayas. ACS Agricultural Science and Technology. 2023 Jul 18;3 (8):694-700. https://doi.org/10.1021/acsagscitech.3c00126

10. MacNeill GJ, Mehrpouyan S, Minow MAA, Patterson JA, Tetlow IJ, Emes MJ. Starch as a source, starch as a sink: The bifunctional role of starch in carbon allocation. J Exp Bot. 2017; 68:4433-53. https://doi.org/10.1093/jxb/erx291

11. Cho YG, Kang KK. Functional analysis of starch metabolism in plants. Plants. 2020;9:p. 1152. https://doi.org/10.3390/plants9091152

12. Huang L, Tan H, Zhang C, Li Q, Liu Q. Starch biosynthesis in cereal endosperms: an updated review over the last decade. Plant Commun. 2021;2: Article 100237. https://doi.org/10.1016/J.XPLC.2021.100237

13. Sahu N, Singh N, Arya KR, Reddy SS, Rai AK, Shukla V et al. Assessment of the dual role of *Lyonia ovalifolia* (Wall.) Drude in inhibiting AGEs and enhancing GLUT4 translocation through LC-ESI-QTOF-MS/MS determination and in silico studies. Frontiers in Pharmacology. 2023 Mar 27;14:1073327. https://doi.org/10.3389/fphar.2023.1073327/

14. Ferrero DML, Diez MD, Kuhn ML, Falaschetti CA, Piattoni CV, Iglesias AA *et al*.On the roles of wheat endosperm ADP-glucose pyrophosphorylase subunits. Front Plant Sci. 2018;9:1498. https://doi.org/10.3389/fpls.2018.01498

15. Hwang SK, Singh S, Maharana J, Kalita S, Tuncel A, Rath T et al. Mechanism underlying heat stability of the rice endosperm cytosolic ADP-glucose pyrophosphorylase. Front Plant Sci. 2019; 10:70. https://doi.org/10.3389/fpls.2019.00070

16. Sun H, Li J, Song H, Yang D, Deng X, Liu J *et al*. Comprehensive analysis of AGPase genes uncovers their potential roles in starch biosynthesis in lotus seed. BMC Plant Biol. 2020; 20:1-15. https://doi.org/10.1186/S12870-020-02666-Z

17. Gadewar M, Prashanth GK, Babu MR, Dileep MS, Prashanth PA, Rao S *et al*. Unlocking nature's potential: Green synthesis of ZnO nanoparticles and their multifaceted applications- A concise overview. Journal of Saudi Chemical Society. 2023 Nov 25; 101774. https://doi.org/10.1016/j.jscs.2023.101774

18. Kim KH, Kim JY. Understanding wheat starch metabolism in properties, environmental stress condition and molecular approaches for value-added utilization. Plants (Basel). 2021;25:10 (11):2282. https://doi.org/10.3390/plants10112282 PMID: 34834645; PMCID: PMC8624758.

19. Begcy K, Sandhu J, Walia H. Transient heat stress during early seed development primes germination and seedling establishment in rice. Front Plant Sci. 2018;9:1768. https://doi.org/10.3389/fpls.2018.01768

20. Goel S, Singh M, Grewal S, Razzaq A, Wani SH. Wheat proteins: a valuable resources to improve nutritional value of bread. Frontiers in Sustainable Food Systems. 2021 Nov 17;5:769681. https://doi.org/10.3389/fsufs.2021.769681

21. Molero G, Joynson R, Pinera-Chavez FJ, Gardiner LJ, Rivera-Amado C, Hall A, Reynolds MP. Elucidating the genetic basis of biomass accumulation and radiation use efficiency in spring wheat and its role in yield potential. Plant Biotechnol J. 2019;17:1276-88. https://doi.org/10.1111/pbi.13052

22. Rivera-Amado C, Trujillo-Negrellos E, Molero G, Reynolds MP, Sylvester-Bradley R, Foulkes MJ. Optimizing dry-matter partitioning for increased spike growth, grain number and harvest index in spring wheat. Field Crops Res. 2019;240:154-67. https://doi.org/10.1016/j.fcr.2019.04.016

23. Quintero A, Molero G, Reynolds MP, Calderini DF. Trade-off between grain weight and grain number in wheat depends on G×E interaction: A case study of an elite CIMMYT panel (CIMCOG). European J Agro. 2018;92:17-29. https://doi.org/10.1016/j.eja.2017.09.007

24. Rajak BK, Rani P, Singh N, Singh DV. Sequence and structural similarities of ACCase protein of Phalaris minor and wheat: An insight to explain herbicide selectivity. Frontiers in Plant Science. 2023a Jan 4;13:1056474. https://doi.org/10.3389/fpls.2022.1056474

25. Rajak BK, Rani P, Mandal P, Chhokar RS, Singh N, Singh DV. Emerging possibilities in the advancement of herbicides to combat acetyl-CoA carboxylase inhibitor resistance. Front Agron. 2023b;5(1218824):10-3389. https://doi.org/10.3389/fagro.2023.1218824

26. Griffiths S, Wingen L, Pietragalla J, Garcia G, Hasan A, Miralles D *et al*. Genetic dissection of grain size and grain number trade-offs in CIMMYT wheat germplasm. PLoS ONE. 2015; 10: e0118847. https://doi.org/10.1371/journal.pone.0118847

27. Malik C, Dwivedi S, Rabuma T, Kumar R, Singh N, Kumar A *et al*. De novo sequencing, assembly and characterization of *Asparagus racemosus* transcriptome and analysis of expression profile of genes involved in the flavonoid biosynthesis pathway. Frontiers in Genetics. 2023;14. https://doi.org/10.3389/fgene.2023.1236517

28. Brinton J, Simmonds J, Minter F, Leverington-Waite M, Snape J, Uauy C. Increased pericarp cell length underlies a major quantitative trait locus for grain weight in hexaploid wheat. New Phytol. 2017;215(3):1026-38. https://doi.org/10.1111/nph.14624 Epub 2017 Jun 2. PMID: 28574181.

29. Wang W, Simmonds J, Pan Q, Davidson D, He F, Battal A *et al*. Gene editing and mutagenesis reveal inter-cultivar differences and additivity in the contribution of TaGW2 homoeologues to grain size and weight in wheat. Theor Appl Genet. 2018;131 (11):2463-75. https://doi.org/10.1007/s00122-018-3166-7

30. Sahariah P, Bora J, Malik S, Syiem D, Bhan S, Hussain A *et al*. Therapeutic potential of *Dillenia indica* L. in attenuating hyperglycemia-induced oxidative stress and apoptosis in alloxan-administered diabetic mice. Frontiers in Bioscience-Landmark. 2023 May 26;28(5):105. https://doi.org/10.31083/j.fbl2805105

31. Tillett BJ, Hale CO, Martin JM, Giroux MJ. Genes impacting grain weight and number in wheat (*Triticum aestivum* L. ssp. *aestivum*). Plants (Basel). 2022;4:11(13):1772. https://doi.org/10.3390/plants11131772

32. Zhang Y, Li D, Zhang D, Zhao X, Cao X, Dong L *et al*. Analysis of the functions of TaGW2 homoeologs in wheat grain weight and protein content traits. Plant J. 2018;94(5):857-66. https://doi.org/10.1111/tpj.13903